

p53 suppresses type II endometrial carcinomas in mice and governs endometrial tumour aggressiveness in humans

Peter J. Wild^{1,#}, Kristian Ikenberg¹, Thomas J. Fuchs², Markus Rechsteiner¹, Strahil Georgiev³, , Nicklaus Fankhauser³, Aurelia Noske¹, Matthias Roessle¹, Rosmarie Caduff¹, Athanassios Dellas⁴, Daniel Fink⁵, Holger Moch¹, Wilhelm Krek³ and Ian J. Frew^{6,#,§}

Supporting Information Table of Contents

Supporting Information Materials and Methods	Pages 1-3
Supporting Information Figures 1-10	Pages 4-13
Supporting Information Tables 1 and 2	Pages 14-15

Supporting Information: Materials and Methods

TP53 deep sequencing primers

p53 primers

MID1

p53 Ex.5 F_MID1	5'-CGTATCGCCTCCCTCGCGCCATCAGACGAGTGCGTcacttgtgccctgactttca-3'
p53 Ex.5 R_MID1	5'-CTATGCGCCTTGCCAGCCCGCTCAGACGAGTGCGTaaccagccctgtctct-3'
p53 Ex.5 Fs2_MID1	5'-CGTATCGCCTCCCTCGCGCCATCAGACGAGTGCGTcagctgtgggtgattcca-3'
p53 Ex.5 Rs1_MID1	5'-CTATGCGCCTTGCCAGCCCGCTCAGACGAGTGCGTtcatgtgctgtgactgcttg-3'
p53 Ex.6 F_MID1	5'-CGTATCGCCTCCCTCGCGCCATCAGACGAGTGCGTcaggcctctgattcctcact-3'
p53 Ex.6 R_MID1	5'-CTATGCGCCTTGCCAGCCCGCTCAGACGAGTGCGTtctaaccctcctcccagag-3'
p53 Ex.7 F_MID1	5'-CGTATCGCCTCCCTCGCGCCATCAGACGAGTGCGTccacaggttcccccaagg-3'
p53 Ex.7 R_MID1	5'-CTATGCGCCTTGCCAGCCCGCTCAGACGAGTGCGTcagcaggccaggtgag-3'

MID2

p53 Ex.5 F_MID2	5'-CGTATCGCCTCCCTCGCGCCATCAGACGCTCGACAcacttgtgccctgactttca-3'
p53 Ex.5 R_MID2	5'-CTATGCGCCTTGCCAGCCCGCTCAGACGCTCGACAaaccagccctgtctct-3'
p53 Ex.5 Fs2_MID2	5'-CGTATCGCCTCCCTCGCGCCATCAGACGCTCGACAacagctgtgggtgattcca-3'
p53 Ex.5 Rs1_MID2	5'-CTATGCGCCTTGCCAGCCCGCTCAGACGCTCGACAtcatgtgctgtgactgcttg-3'
p53 Ex.6 F_MID2	5'-CGTATCGCCTCCCTCGCGCCATCAGACGCTCGACAacagcctctgattcctcact-3'
p53 Ex.6 R_MID2	5'-CTATGCGCCTTGCCAGCCCGCTCAGACGCTCGACAActaaccctcctcccagag-3'
p53 Ex.7 F_MID2	5'-CGTATCGCCTCCCTCGCGCCATCAGACGCTCGACAaccacaggttcccccaagg-3'
p53 Ex.7 R_MID2	5'-CTATGCGCCTTGCCAGCCCGCTCAGACGCTCGACAacagcaggccaggtgag-3'
p53 Ex.8 F_MID2	5'-CGTATCGCCTCCCTCGCGCCATCAGACGCTCGACAagcctctgcttcttttcc-3'
p53 Ex.8 R_MID2	5'-CTATGCGCCTTGCCAGCCCGCTCAGACGCTCGACAaactgcacccttggtctcc-3'

MID3

p53 Ex.5 F_MID3	5'-CGTATCGCCTCCCTCGCGCCATCAGAGACGCACTCacttgtgccctgactttca-3'
p53 Ex.5 R_MID3	5'-CTATGCGCCTTGCCAGCCCGCTCAGAGACGCACTCaaccagccctgtctct-3'
p53 Ex.5 R_MID3_short*	5'-CTATGCGCCTTGCCAGCCCGCTCAGAGACGCACTCctgtctaccatcgctatctg-3'
p53 Ex.5 Fs2_MID3	5'-CGTATCGCCTCCCTCGCGCCATCAGAGACGCACTCacagctgtgggtgattcca-3'
p53 Ex.5 Rs1_MID3	5'-CTATGCGCCTTGCCAGCCCGCTCAGAGACGCACTCtcatgtgctgtgactgcttg-3'
p53 Ex.6 F_MID3	5'-CGTATCGCCTCCCTCGCGCCATCAGAGACGCACTCcaggcctctgattcctcact-3'
p53 Ex.6 R_MID3	5'-CTATGCGCCTTGCCAGCCCGCTCAGAGACGCACTCctaaccctcctcccagag-3'
p53 Ex.7 F_MID3	5'-CGTATCGCCTCCCTCGCGCCATCAGAGACGCACTCccacaggttcccccaagg-3'
p53 Ex.7 R_MID3	5'-CTATGCGCCTTGCCAGCCCGCTCAGAGACGCACTCcagcaggccaggtgag-3'
p53 Ex.8 F_MID3	5'-CGTATCGCCTCCCTCGCGCCATCAGAGACGCACTCgcctctgcttcttttcc-3'
p53 Ex.8 R_MID3	5'-CTATGCGCCTTGCCAGCCCGCTCAGAGACGCACTCtaactgcacccttggtctcc-3'

MID4

p53 Ex.8 F_MID4**	5'-CGTATCGCCTCCCTCGCGCCATCAGAGCACTGTAGgcctctgcttcttttcc-3'
p53 Ex.8 R_MID4**	5'-CTATGCGCCTTGCCAGCCCGCTCAGAGCACTGTAGtaactgcacccttggtctcc-3'

*MID3_short primer combination was used with Fs2 for p53 exon 5 amplification due to better PCR performance

**MID4 primer combinations were used instead of MID1 in p53 exon 8 multiplexing due to better PCR performance

Statistical determination of risk score based on analysis of multiple immunohistochemical variables

One of the major statistical challenges in large scale immunohistochemical studies are missing values in the design matrix due to missing or corrupt spots on the TMA. The more markers that are investigated the higher the chance that at least one value is missing per patient. Frequently this problem is tackled by either sacrificing a larger number of patient records or by employing unreliable multiple imputation techniques. In this study, ignoring missing values would reduce the set of patients with all measurements from 410 to 302. To overcome this problem we developed a novel statistical approach based on a learning model that is invariant to missing values and results in an easily interpretable and practically applicable linear model. Prognostic power of the individual and combined clinico-pathologic variables was assessed by learning univariate proportional hazard models, yielding eight markers significantly associated with overall survival. To correct for multiple testing, the false discovery rate (FDR) procedure was applied with a FDR of 0.01, reducing the set of significantly associated markers to four. A risk score was calculated for each patient by a linear combination of the univariate Cox regression coefficients β and the corresponding IHC measurements $x = \{x_1, x_2, \dots, x_D\}$, where D is the number of markers in the signature. Single x_i might be unavailable due to missing TMA spots. Finally, the score was normalized by the number of markers measured:

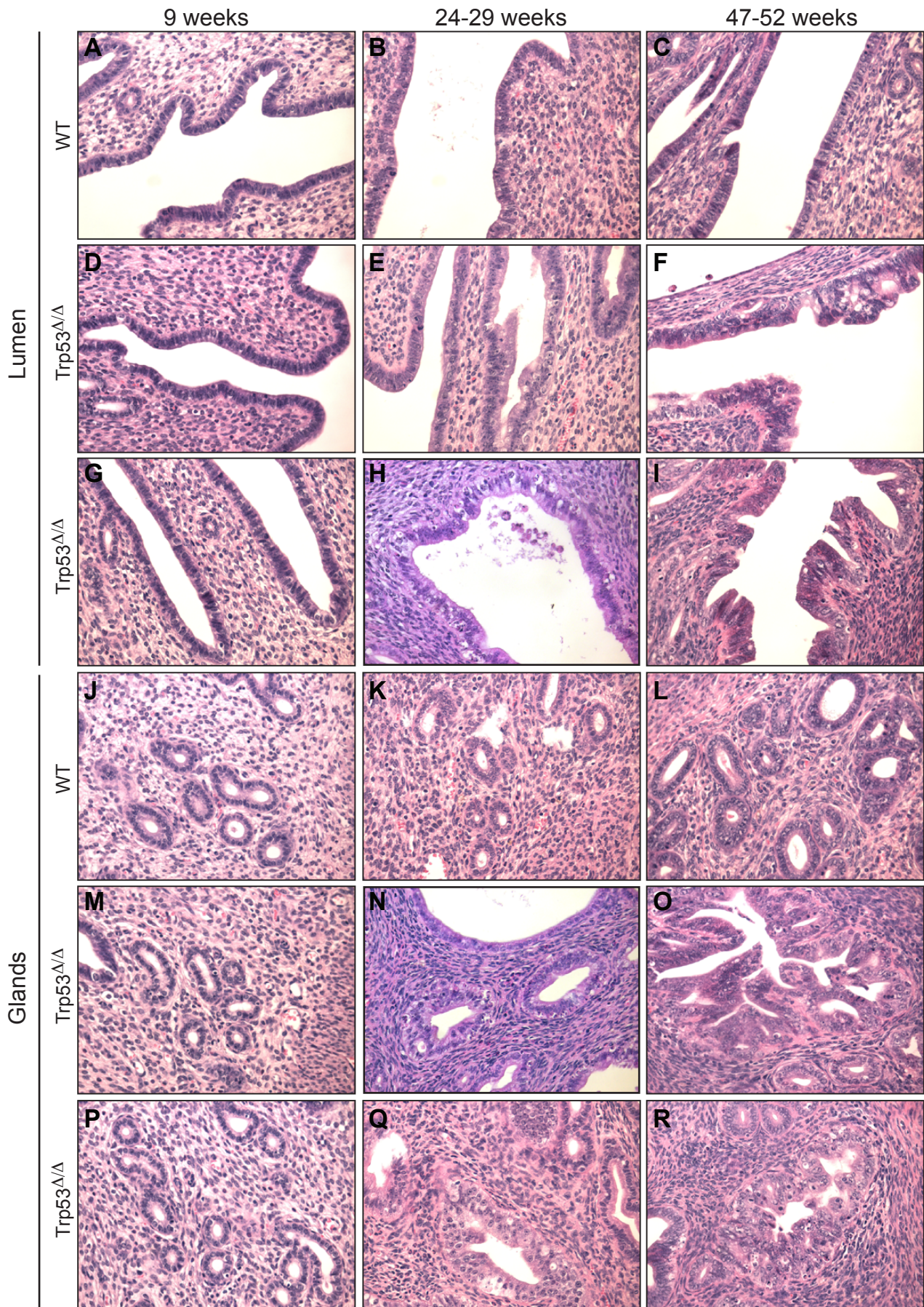
$$\text{score}(x) = \left(\sum_{i=1}^D (\beta_i x_i) \alpha_i \right) \left/ \left(\sum_{i=1}^D \alpha_i \right) \right., \quad \alpha_i = \begin{cases} 1, & \text{if } x_i \text{ exists} \\ 0, & \text{if } x_i \text{ is missing} \end{cases}$$

Based on this risk score, patients were assigned to a high risk group and a low risk group, split at the 50th percentile (median) of all scores. Thus, the final model consisted of the coefficient vector β and the median threshold θ . The model was thoroughly evaluated with cross validation experiments and a multivariate Cox regression analysis. The cross validation experiments were conducted as follows:

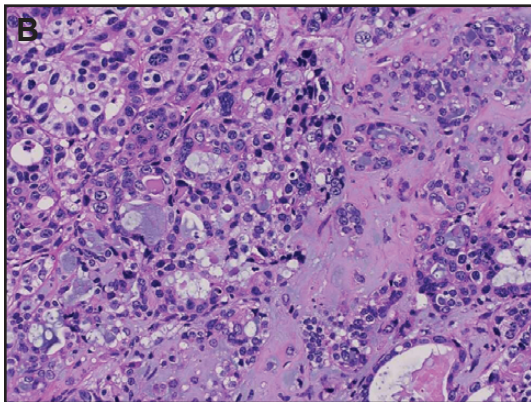
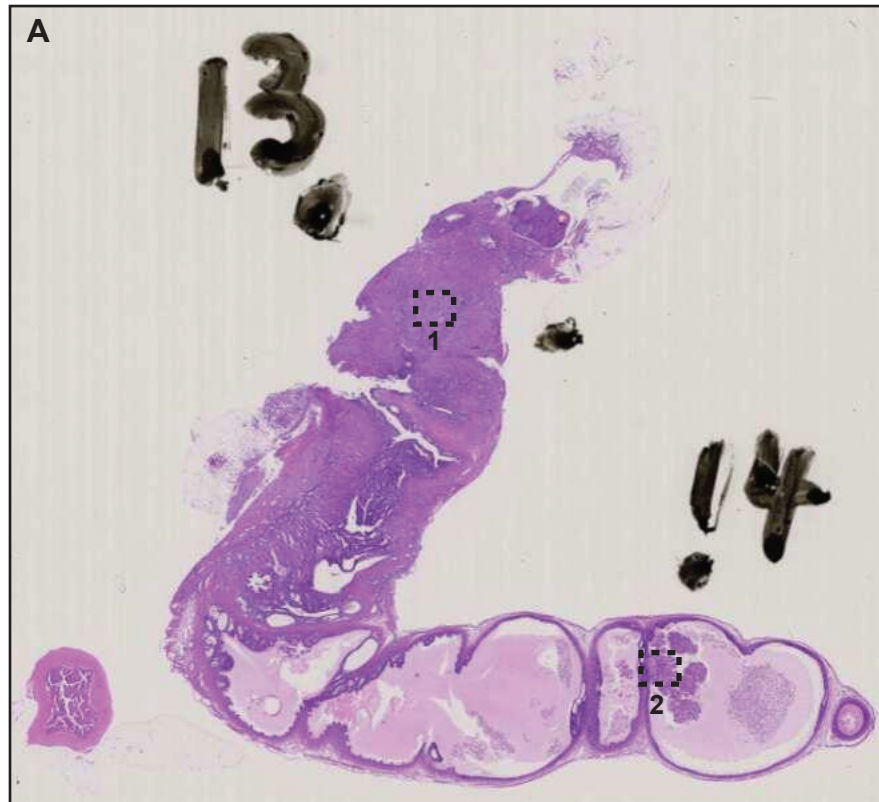
1. Divide the patients into K cross-validation folds (groups) at random.

2. For each fold $k = 1, 2, \dots, K$
 - a. Find a subset of univariate statistically significant (LRT $p < 0.05$) predictors for the overall survival, using all of the patients except those in fold k .
 - b. Filter the selected predictors based on a FDR of 0.01.
 - c. Using just this subset of predictors, build a multivariate linear model using the formulation in score equation, using all of the patients except those in fold k .
 - d. Use the model to predict the score for the patients in fold k .
3. Aggregate the out-of-bag predictions of all patients and split them in two groups based on the median predicted score.
4. Calculate the Kaplan-Meier estimator for each group and report the LRT p -value of their difference in survival expectation.

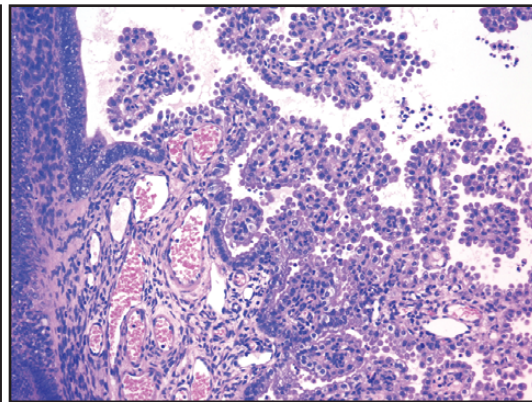
10-fold cross validation was conducted by partitioning the dataset into 10 parts of equal size using 90% of the patients for learning and 10% for validation. The procedure was repeated 10 times resulting in a 10-fold score for each patient. The resulting differentiation between high risk and low risk patient was still highly significant as shown in Fig. 6C ($p=0.000011$).



Supporting Information Figure 1 Representative histological appearances of luminal (A-J) and glandular (J-R) endometria in wild type (A-C, J-L) and Trp53 Δ/Δ (D-I, M-R) mice. Pictures are representative of cohorts of mice aged 9 weeks (A,D,G,J,M,P), 24-29 weeks (B,E,H,K,N,Q) or 47-52 weeks (C,F,I,L,O,R).

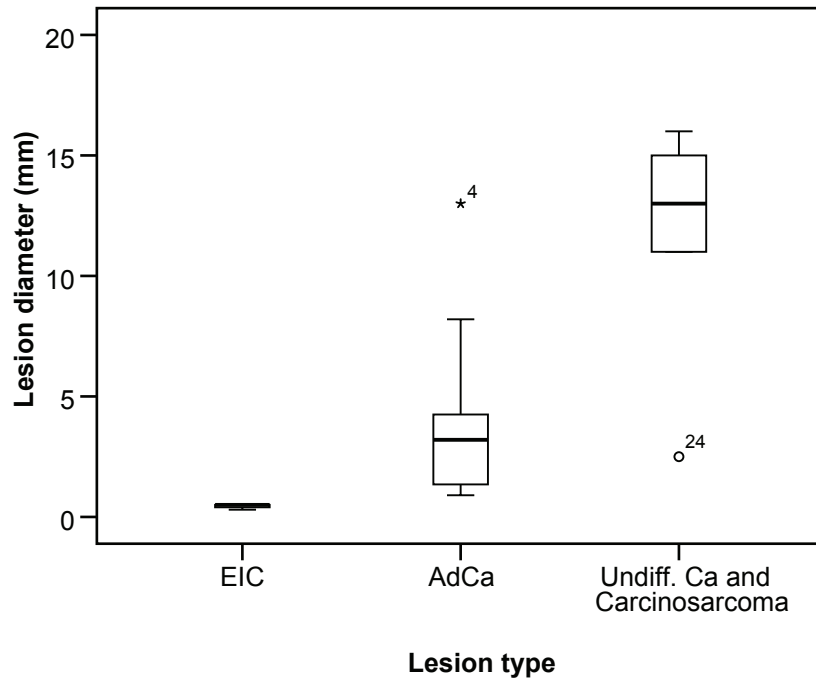


Box 1, Carcinosarcoma

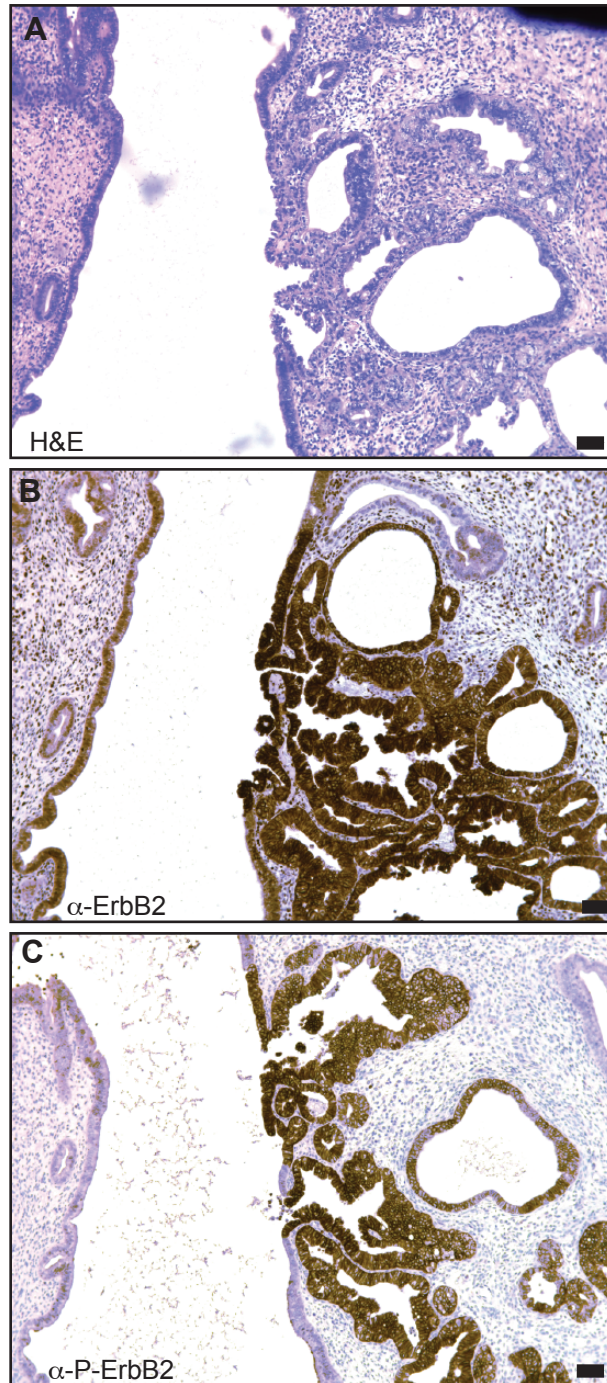


Box 2, Serous adenocarcinoma (papillary)

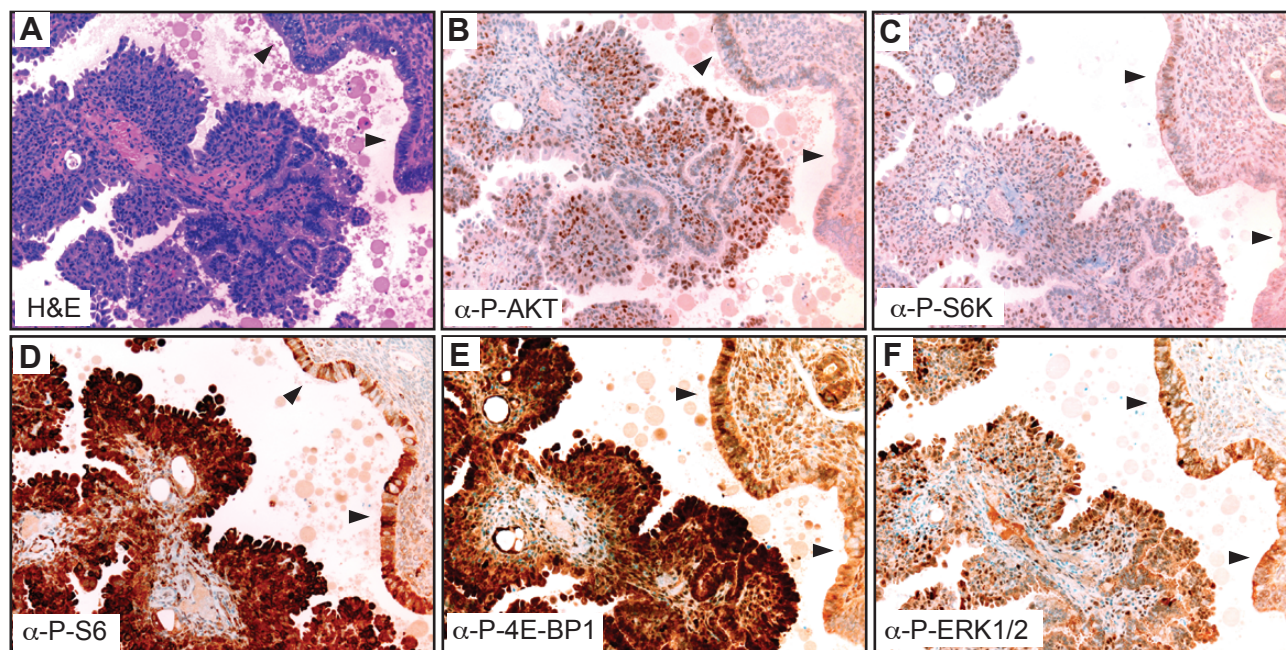
Supporting Information Figure 2 Example of a carcinosarcoma and of a serous, partly clear cell adenocarcinoma arising in the uterus of a 68 week-old *Trp53 Δ/Δ* mouse. (A) Low power magnification of a longitudinal cross section of the uterus, displaying the carcinosarcoma in the upper uterine branch and a papillary serous, partly clear cell adenocarcinoma in the lower uterine branch. (B) Zoom of the region from box 1 in A showing a mixed clear cell adenocarcinoma and chondrosarcoma phenotype. (C) Zoom of the region from box 2 in A showing a papillary serous and partly clear cell adenocarcinoma.



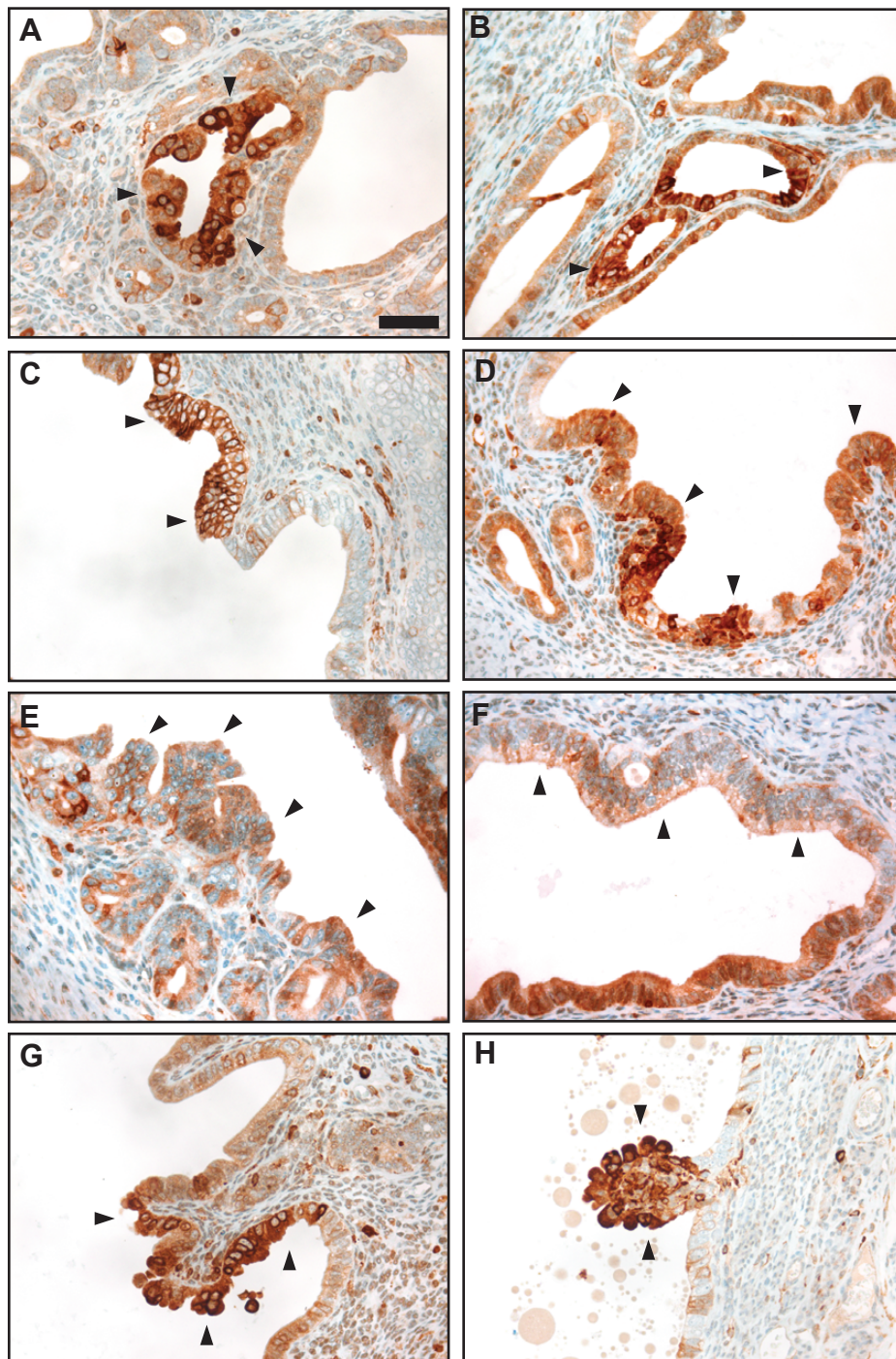
Supporting Information Figure 3 Sizes of lesions in *Trp53* mutant mice. Box plot showing the maximum diameter (mm) of lesions identified in mice aged 58-72 weeks, grouped according to lesion type. EIC: endometrial intraepithelial carcinoma, AdCa: adenocarcinoma, Undiff. Ca and Carcinosarcoma: undifferentiated carcinoma and carcinosarcoma.



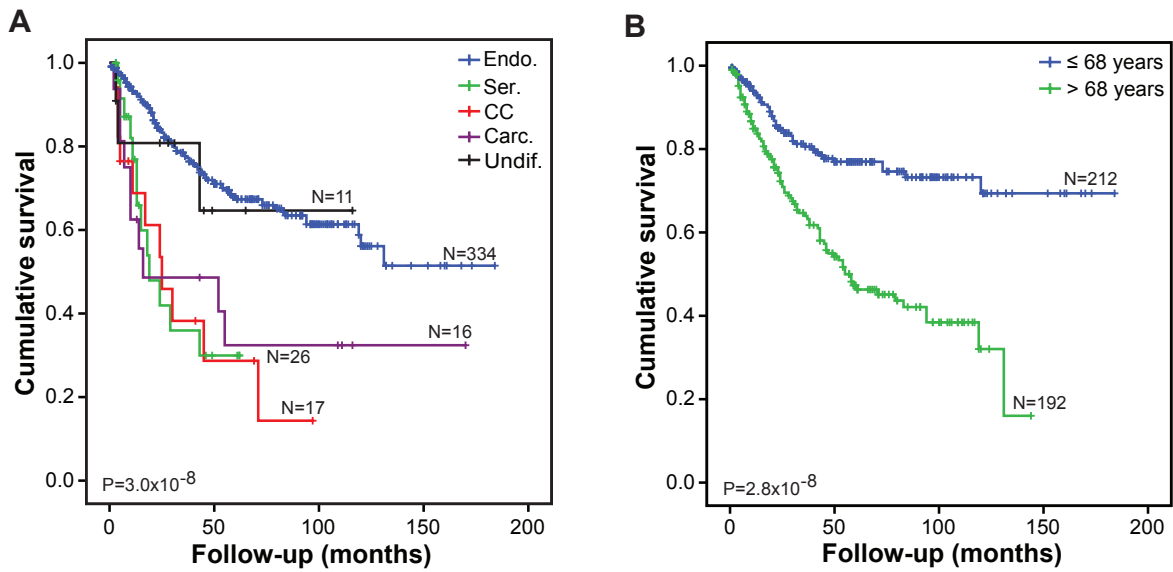
Supporting Information Figure 4 Activation of ErbB2 in a tumour from a *Trp53* mutant mouse. (A) Haemotoxlin and eosin stain of a clear cell EIC lesion. (B) Immunohistochemical staining using an antibody against ErbB2. (C) Immunohistochemical staining using an antibody against phospho-Tyr1248-ErbB2, a marker of ErbB2 activation. This staining is classified as DAKO 3+ on the Hercep test criteria. Scale bars represent 200 μ m.



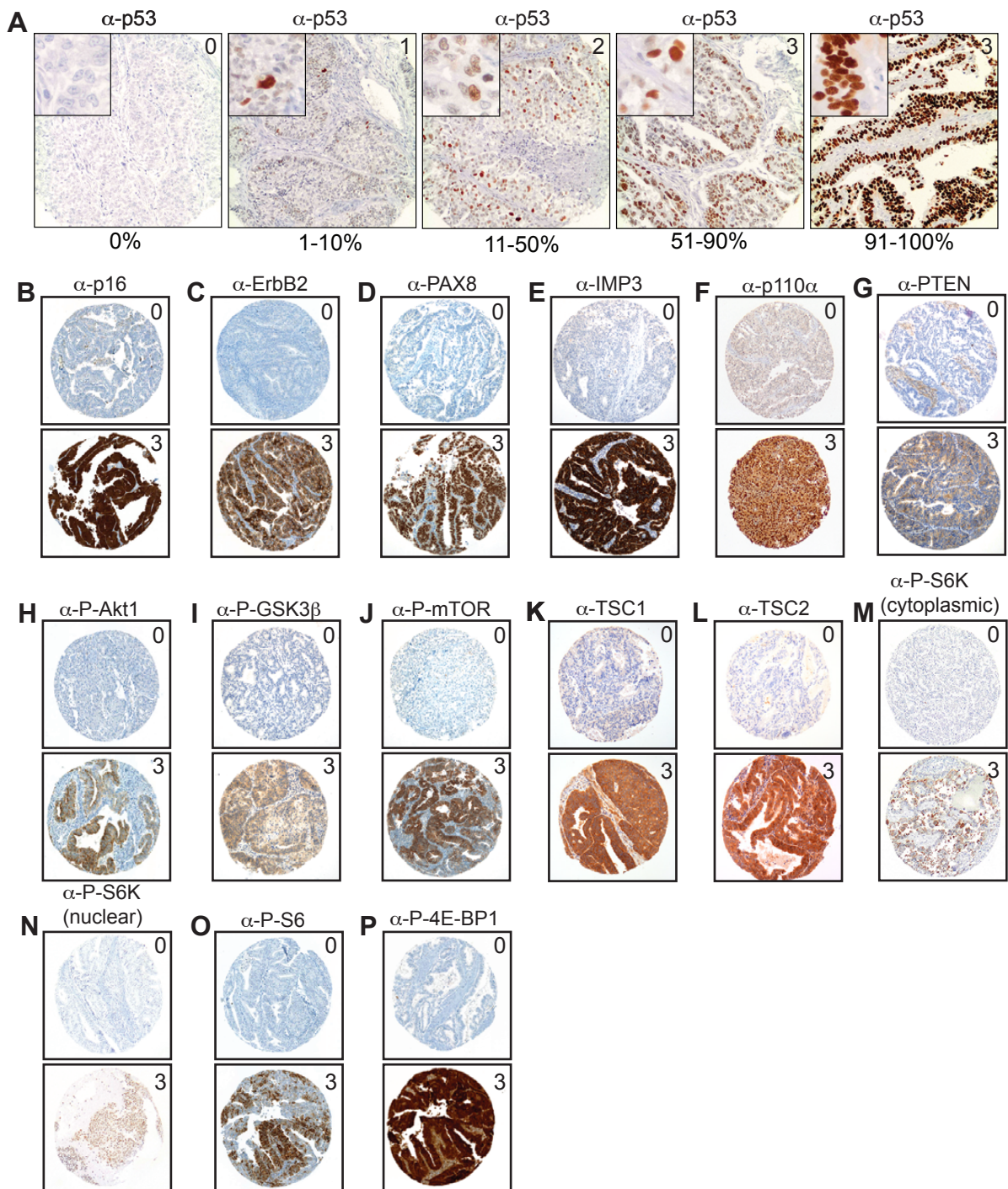
Supporting Information Figure 5 Activation of the PI3K-AKT-mTOR signalling pathway in a tumour from a *Trp53* mutant mouse. Adjacent sections of a serous adenocarcinoma were stained with (A) haematoxylin and eosin or immunohistochemically with antibodies against (B) phospho-Ser473-AKT, (C) phospho-Thr421/Ser424-p70 S6 Kinase, (D) phospho-Ser240/244-ribosomal S6 protein, (E) phospho-Thr37/46-4E-BP1, (F) phospho-Thr202/Tyr204-ERK1/2. Arrowheads depict the normal-appearing, non-dysplastic surface epithelium adjacent to the tumour.



Supporting Information Figure 6 Upregulation of P-S6 at discrete early lesions in *Trp53* mutant mice. (A-H) Immunohistochemical staining of various early lesions using an antibody against phospho-Ser240/244-ribosomal S6 protein. (A,B) Examples of upregulated expression in endometrial glandular dysplasia arising in glands. (C,D) Examples of upregulated expression in endometrial glandular dysplasia arising in luminal surface epithelium. (E,F) Examples of endometrial glandular dysplasia that do not show elevated staining. (G,H) Upregulation P-S6 expression was observed in all very early papillary endometrial intraepithelial carcinoma lesions. Arrowheads in A-F highlight regions of endometrial glandular dysplasia and in G,H sites of papillary endometrial intraepithelial carcinoma. All images are the same magnification, scale bar represents 50 μ m.

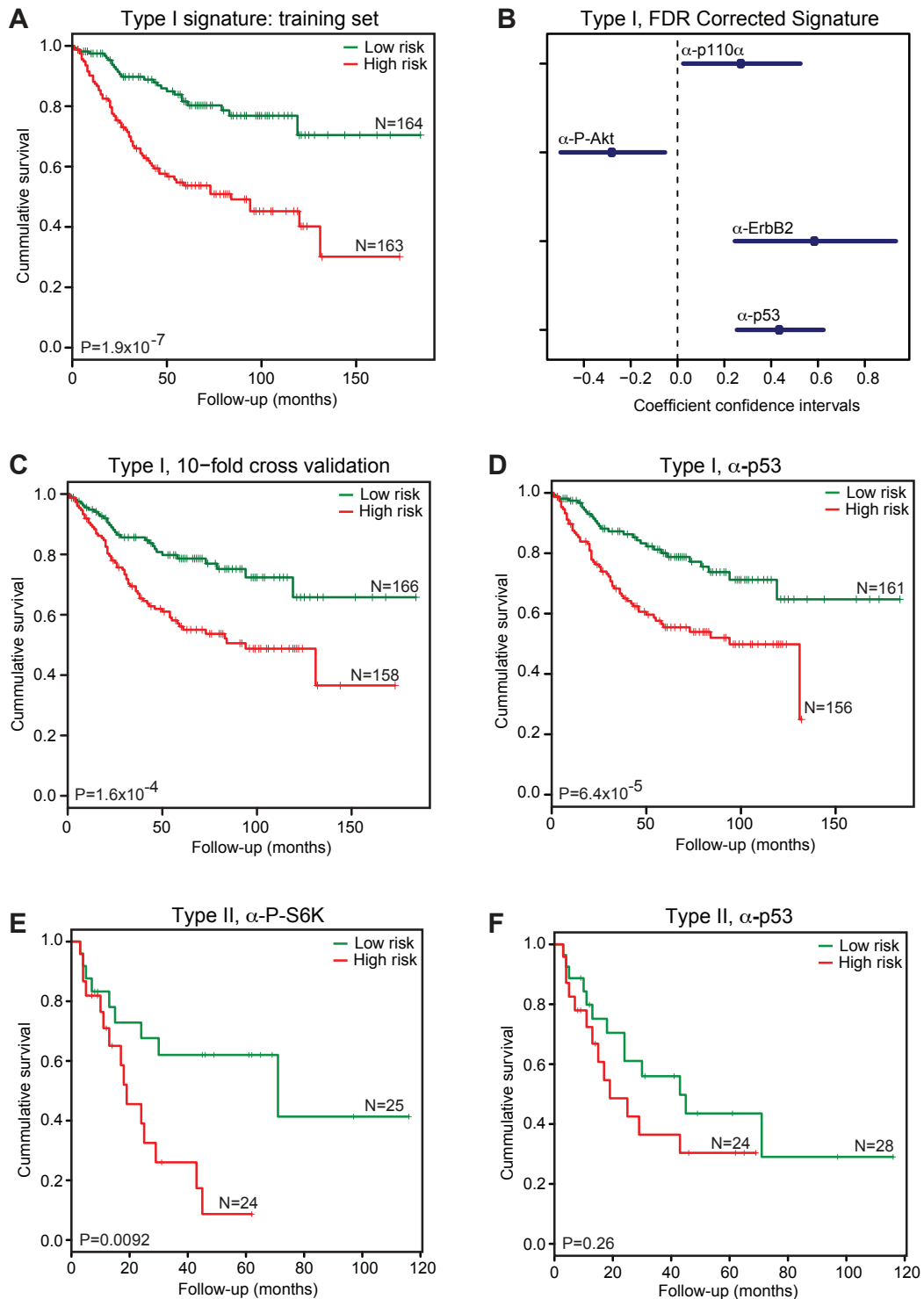


Supporting Information Figure 7 Patient survival correlated to clinical parameters. Kaplan-Meier plots of patient survival over time after diagnosis when patients were grouped according to histologic tumour subtype (**A**) or age at diagnosis (**B**). P values are from the Log Rank (Mantel-Cox) test to test the equality of survival distributions of each group. Abbreviations: Endo. endometrioid carcinoma, Ser. serous carcinoma, CC. clear cell carcinoma, Carc. carcinosarcoma, Undif. undifferentiated carcinoma.

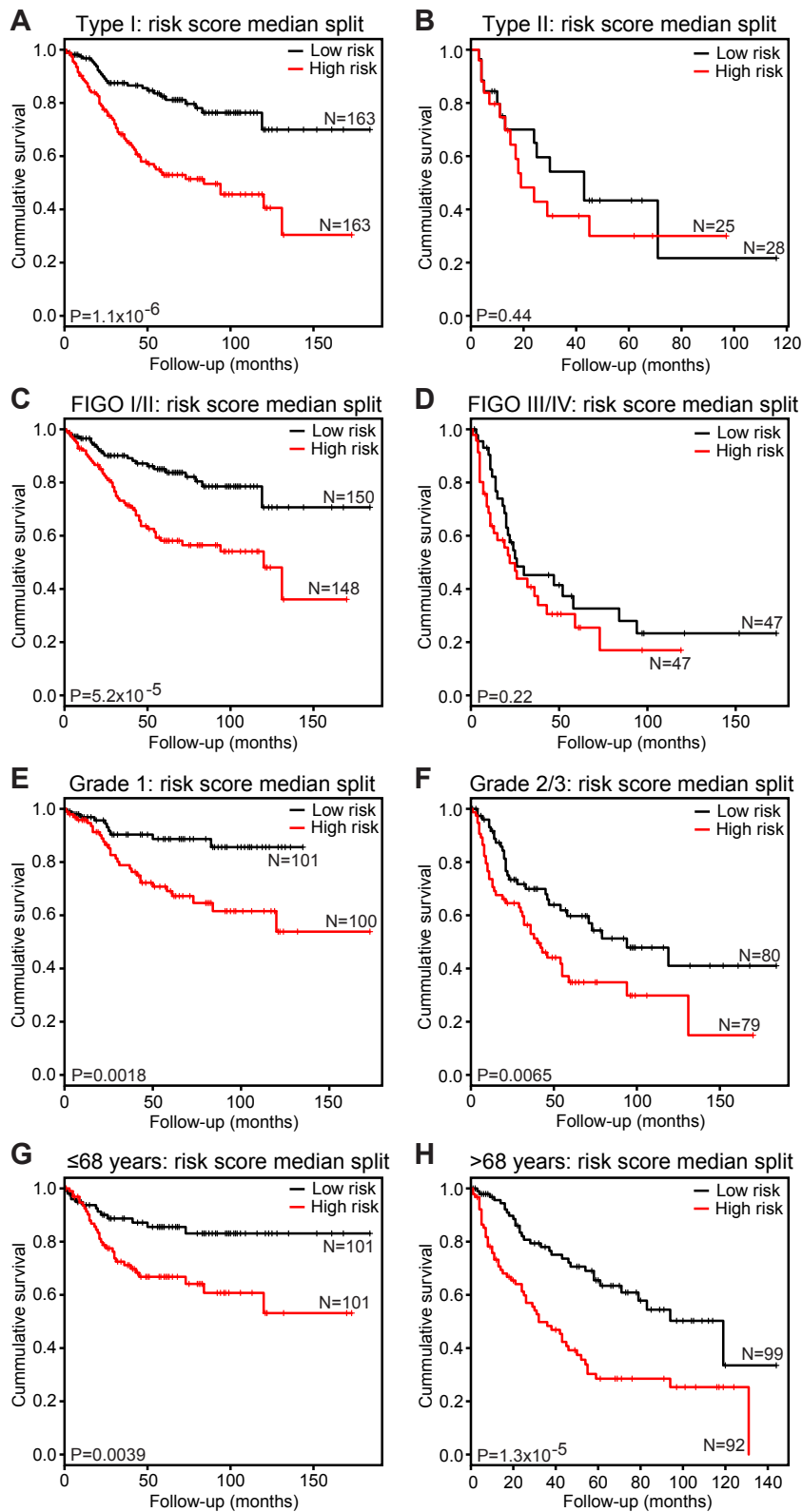


Supporting Information Figure 8

(A) Examples of representative TMA spots (inset is zoom) showing different p53 IHC staining patterns classified according to frequency of cells exhibiting strong nuclear immunoreactivity. Cells were classified in 4 groups (IHC score 0-3) for analysis in Fig 4 and in 5 groups (IHC score as % groups) for analysis in all other Figures. (B-N) Examples of TMA spots with negative (score 0) and strongly positive (score 3) immunoreactivity for antibodies against p16 (B), ErbB2 (C), PAX8 (D), IMP3 (E), p110 α (F), PTEN (G), phospho-Ser473-AKT (H), phospho-Ser9-GSK3 β (I), phospho-Ser2448-mTOR (J), TSC1 (K), TSC2 (L), phospho-Thr421/Ser424-p70 S6 Kinase (cytoplasmic staining) (M), phospho-Thr421/Ser424-p70 S6 Kinase (nuclear staining) (N), phospho-Ser240/244-ribosomal S6 protein (O) and phospho-Thr37/46-4E-BP1 (P).



Supporting Information Figure 9 Kaplan-Meier plots based on risk-model analysis of survival of patients with type I endometrial carcinomas (A-D) or type II carcinomas (E,F). (A) Patient stratification using a risk-model four-marker signature based on staining patterns for p110 α , phospho-Ser473-AKT, ErbB2 and p53. (B) Contribution of each marker to the signature represented by coefficients and confidence intervals. (C) Patient stratification based on 10-fold cross-validation of the linear risk score model. (D) Patient stratification based on the median split of p53 expression frequency only, showing equal prognostic power to the four-marker model. (E) Patient stratification in type II tumours based on the median split of phospho-Thr421/Ser424-p70 S6 Kinase nuclear staining. (F) Patient stratification in type II tumours based on the median split of p53 staining frequency. Log Rank (Mantel-Cox) tests were conducted to test for equality in the survival expectation of both groups. N values represent the number of patients in each group.



Supporting Information Figure 10 Kaplan-Meier plots for high-risk and low-risk endometrial carcinoma patients based on the four-marker signature consisting of p110 α , phospho-Ser240/244-ribosomal S6 protein, ErbB2 and p53. (A) Kaplan-Meier plots for subgroups of patients based on low and high risk scores in type I tumours, (B) in type II tumours, (C) in FIGO stage I and II tumours, (D) in FIGO stage III and IV tumours, (E) in grade 1 tumours, (F) in grade 2 and 3 tumours, (G) in tumours arising in patients 68 years or younger or (H) in tumours arising in patients older than 68 years, respectively. Log Rank (Mantel-Cox) tests were conducted to test for equality in the survival expectation of both groups. N values represent the number of patients in each group.

Supporting Information Table 1. Clinicopathologic and immunohistochemical features in endometrial cancer patients

<i>Variable</i>	<i>n</i>	<i>%</i>	<i>Variable</i>	<i>n</i>	<i>%</i>
Follow-up data:			Immunohistochemical data (continued):		
No. of patients	521		Nuclear p110 α (intensity)		
No. of patients with follow-up (%)	410 (78.7%)		negative	21	4.0
Median follow-up (range)	38 months (1-184 months)		score 1+	141	27.1
Clinicopathological characteristics:			score 2+	163	31.3
Age at diagnosis (median 68 years, range 33-92)			score 3+	120	23.0
\geq 68 years	268	51.4	unknown	76	14.6
> 68 years	252	48.4	Cytoplasmic PTEN (intensity)		
unknown	1	0.2	negative	353	67.8
FIGO stage			score 1+	63	12.1
I	263	50.5	score 2+	41	7.9
II	65	12.5	score 3+	8	1.5
III	76	14.6	unknown	56	10.7
IV	18	3.5	Cytoplasmic P-Akt1 (Ser473) (intensity)		
unknown	99	19.0	negative	135	25.9
Histologic subtype			score 1+	177	34.0
Endometrioid adenocarcinoma	436	83.7	score 2+	124	23.8
Serous adenocarcinoma	34	6.5	score 3+	43	8.3
Clear cell adenocarcinoma	19	3.6	unknown	42	8.1
Undifferentiated carcinoma	16	3.1	Cytoplasmic P-GSK3 β (intensity)		
Carcinosarcoma	16	3.1	negative	391	75.0
unknown	0	0	score 1+	55	10.6
Grading FIGO			score 2+	15	2.9
1	270	51.8	score 3+	3	0.6
2	128	24.6	unknown	57	10.9
3	88	16.9	Cytoplasmic P-mTOR (intensity)		
unknown	35	6.7	negative	182	34.9
Immunohistochemical data:			score 1+	135	25.9
Nuclear p53 (%)			score 2+	114	21.9
negative	231	44.3	score 3+	43	8.3
1-10%	129	24.8	unknown	47	9.0
11-50%	50	9.6	Cytoplasmic P-S6K (intensity)		
51-90%	28	5.4	negative	397	76.2
91-100%	44	8.4	score 1+	45	8.6
unknown	39	7.5	score 2+	13	2.5
Cytoplasmic p16 (intensity)			score 3+	4	0.8
negative	51	9.8	unknown	62	11.9
score 1+	160	30.7	Nuclear P-S6K (intensity)		
score 2+	211	40.5	negative	252	48.4
score 3+	41	7.9	score 1+	144	27.6
unknown	58	11.1	score 2+	58	11.1
ErbB2 (Dako HercepTest criteria)			score 3+	4	0.8
negative	391	75.0	unknown	63	12.1
score 1+	55	10.6	Cytoplasmic P-S6 ribosomal protein (Ser235/236) (intensity)		
score 2+	9	1.7	negative	251	48.2
score 3+	10	1.9	score 1+	87	16.7
unknown	56	10.7	score 2+	82	15.7
Nuclear PAX8 (intensity)			score 3+	50	9.6
negative	74	14.2	unknown	51	9.8
score 1+	127	24.4	Cytoplasmic P-4E-BP1 (Thr37/46) (intensity)		
score 2+	173	33.2	negative	110	21.1
score 3+	94	18.0	score 1+	86	16.5
unknown	53	10.2	score 2+	196	37.6
Cytoplasmic IMP3 (intensity)			score 3+	96	18.4
negative	269	51.6	unknown	33	6.3
score 1+	90	17.3	Cytoplasmic TSC1		
score 2+	64	12.3	negative	14	2.7
score 3+	38	7.3	score 1+	77	14.8
unknown	60	11.5	score 2+	213	40.9
			score 3+	95	18.2
			unknown	122	23.4
			Cytoplasmic TSC2		
			negative	114	21.9
			score 1+	155	29.8
			score 2+	88	16.9
			score 3+	17	3.3
			unknown	147	28.2

